Speciation-Dependent Toxicity of Neptunium(V) Toward *Chelatobacter heintzii*

JAMES E. BANASZAK,[†,‡]
DONALD T. REED,*,[‡] AND
BRUCE E. RITTMANN[†]

*Department of Civil Engineering, Northwestern University,
2145 Sheridan Road, Evanston, Illinois 60208-3109, and
Chemical Technology Division, Argonne National Laboratory,
9700 South Cass Avenue, Argonne, Illinois 60439*

This work investigates how chemical speciation controls the toxicity of neptunium and the neptunium–NTA complex toward *Chelatobacter heintzii.* We studied the effect of aquo and complexed/precipitated neptunium on the growth of *C. heintzii* in noncomplexing glucose and phosphate-buffered nitrilotriacetic acid (NTA) growth media. Equilibrium chemical speciation modeling and absorption spectroscopy were used to link neptunium speciation to biological growth inhibition. Our results show that metal toxicity of aquo NpO_2^+ significantly limits the growth of *C. heintzii* at free metal ion concentrations greater than $\approx 10^{-5}$ M. However, neptunium concentrations $\geq 10^{-4}$ M do not cause measurable radiotoxicity effects in *C. heintzii* when present in the form of a neptunium–NTA complex or colloidal/precipitated neptunium phosphate. The neptunium–NTA complex, which is stable under aerobic conditions, is destabilized by microbial degradation of NTA. When phosphate was present, degradation of NTA led to the precipitation of a neptunium-phosphate phase.

Introduction

Past practices at U.S. Department of Energy (DOE) facilities have resulted in the contamination of subsurface aquifers with mixtures of organic compounds and radionuclides. An important class of mixed contaminants includes co-disposed actinides and organic chelating agents, such as nitrilotriacetic acid (NTA) (*1*). The presence of strong complexing agents in subsurface environments can increase dissolved actinide concentrations, leading to enhanced radionuclide migration in groundwater (*2–4*).

It has recently become clear that microorganisms play an important role in subsurface environmental chemistry (*5*). Microbial activities affect the concentration of biodegradable compounds and redox conditions in subsurface aquifers. Furthermore, microbial degradation of primary substrates in many cases produces or consumes acid equivalents, lowering or raising system pH (*6*). Therefore, the chemical speciation of redox and acid/base-sensitive compounds in groundwaters can be largely dependent on biological activities.

NTA is utilized by some bacteria, including *Chelatobacter heintzii*, as a sole source of carbon, nitrogen, and energy (*7*).

* Corresponding author e-mail: reedd@cmt.anl.gov; phone: 630-252-7964; fax: 630-252-4176.
† Northwestern University.
‡ Argonne National Laboratory.

Degradation of NTA by microorganisms decreases chelate availability, which modifies the speciation of metals and actinides in the system (*8*). The actinide species may form complexes with other ligands in the system; sorb onto oxides, organic matter, or microbial cell membranes; or precipitate from solution (*9, 10*).

The speciation of actinides in the subsurface, after the microbiological degradation of the organic complexant, is defined by the inorganic (e.g., phosphate, carbonate, hydroxy) and organic (humic/fulvic acids) anions present as well as pH. Of particular relevance to this paper, phosphates control metal solubility in some subsurface environments (*11*). In neutral-to-alkaline waters, phosphate complexation can dominate neptunium speciation when phosphate concentrations are $\geq 10^{-4}$ M (*12*), and phosphate additions can decrease neptunium solubility in synthetic groundwaters (*13*). Bioprecipitation of uranium as a phosphate phase was linked to phosphatase–enzyme activity in a *Citrobacter* sp., suggesting that biologically mediated phosphate precipitation may be an effective method of removing actinides from contaminated waters (*14–16*).

Radioactive elements, such as actinides, are unique because they are potentially toxic to microorganisms via two distinct mechanisms. First, actinide species can be chemically toxic, similar to other metals. The uncomplexed metal ions usually are more toxic to microorganisms than are complexed metal species (*17–20*). Neptunium may inhibit growth in the same manner as other metals, for example, by binding with proteins necessary for substrate transport or by substitution into cofacter metal ion sites (*18*). Second, microorganisms are susceptible to toxic effects caused by the ionizing radiation emitted during radioactive decay (*21–23*). Ionizing radiation induces toxicity by causing unrepairable cell damage that prevents cell reproduction or causes cell death via several potential pathways. Reed et al. (*24*) found that radiotoxicity effects of plutonium were induced below the absorbed dose threshold due to intimate association of the plutonium with *C. heintzii*. Neptunium, primarily an α-particle emitter (*25*), is potentially radiotoxic to microorganisms if α-particles emitted interact directly with the cell when the radionuclide is ingested by the organism during metabolic processes (*23*), is present in high enough concentrations to give overall radiation doses that exceed the organism's radiation threshold (*22*), or is sorbed extracellularly (*24*).

As part of our continuing investigations of the interactions between actinide species and microorganisms, we explored the potential toxicity mechanisms of neptunium toward *C. heintzii* and established the stability of the neptunium–NTA complex in the presence of aerobic microbiological activity. We report here that only the free NpO_2^+ ion inhibited growth of *C. heintzii* and that the toxic effects were mitigated when neptunium was complexed with NTA or phosphate or was bound in a neptunium–phosphate colloid/precipitate.

Experimental Section

Sample Preparation. *Chelatobacter heintzii* (ATCC 29600), an obligately aerobic NTA degrader, was grown in a defined NTA culture medium (*26*) consisting of the following mineral additions (in g/L): K_2HPO_4, 1.606; KH_2PO_4, 0.403; NH_4NO_3, 0.499; $MgSO_4 \cdot 7H_2O$, 0.203; $CaCl_2 \cdot 2H_2O$, 0.0200; $FeCl_3 \cdot 6H_2O$, 0.0027; NTA, 0.999; and NaOH to adjust the pH to 7.0 ± 0.1. Cells were harvested in the log phase of growth (600-nm optical density (OD_{600}) ≈ 0.1), rinsed three times in pH 6.2 ± 0.1 0.01 M PIPES [piperazine-*N,N*-bis(2-ethanesulfonic acid)) solution, concentrated by centrifugation, and resuspended

in 0.01 M PIPES solution to prepare an inoculum with a final OD_{600} of 0.4–0.6.

So that α-scintillation counting could be used to determine total neptunium concentrations and to monitor neptunium partitioning, a stock solution of $\geq$95% isotopic purity (by Ci content of α-particle emitters) was prepared by ion exchange. We did not attempt to control the concentration of ^{233}Pa, the daughter product of ^{237}Np. At equilibrium, its concentration was several orders of magnitude lower than ^{237}Np, and its contribution to the radiolytic dose-to-solution was < 5%. Sterile neptunium–NTA sample vessels were prepared by adding incremental amounts of purified ^{237}Np stock solution, filtered through a 0.2-μm membrane filter, to defined mineral media in 30-mL serum bottles. Three control samples were prepared in a similar manner without the addition of neptunium. The samples were inoculated with the culture described above to obtain a target initial cell density of 0.007 or 0.06 OD_{600}. Chemical equilibrium calculations indicated that the initial dominant neptunium speciation in the medium was 63% NpO_2NTA^{2-}, 24% $NpO_2HPO_4^-$, 10% NpO_2^+, and 2% $NpO_2PO_4^{2-}$. Absorption spectroscopy verified that approximately 90% of the neptunium was present in solution in complexed form. However, $NpO_2PO_4^{2-}$ (988.8 nm) could not be separated spectroscopically from NpO_2NTA^{2-} (990.2 nm) due to peak convolution. Growth in the NTA experiments was limited only by the amount of NTA available as a primary substrate.

Neptunium–glucose experiments were conducted in a minimal glucose growth medium to prevent neptunium complexation with inorganic anions (8). The medium was prepared by addition of 0.942 g/L glucose (dextrose), a known carbon source and electron donor substrate for *C. heintzii* (27), to a 0.01 M PIPES solution. The final pH of the solution was adjusted to 6.0 ± 0.1 before 0.2-μm membrane filter sterilization. Aquo Np(V) samples were then prepared by adding incremental amounts of sterile neptunium stock. The neptunium in the glucose system, based on the absorption spectra, was predominantly (>95%) the aquo NpO_2^+ species throughout the experiment. All growth experiments were performed in the dark at room temperature (21 ± 2 °C) under aerobic conditions.

Sample Analysis. Aliquots of 1 mL were periodically drawn from each vessel and analyzed for biomass production, neptunium speciation, and neptunium–NTA complex stability by measuring the visible light–near infrared (VIS–NIR) absorption spectrum from 575 to 1250 nm using a Varian Cary 5 spectrophotometer. A 0.2-mL subsample was then drawn from each aliquot and added to 10 mL of Ultima Gold scintillation cocktail (Packard); another 0.1-mL subsample was added to 0.9 mL of sterile, deionized water. The remainder of the aliquot was filtered through a 0.2-μm filter, and 0.2 mL of the filtered material was added to a second 10-mL scintillation cocktail. Total neptunium concentrations were determined by α-particle scintillation counting of the unfiltered preparation. The amount of bioassociated neptunium was calculated from the difference in α-particle scintillation counts between the unfiltered and filtered samples. All counting was done with a Packard model 2500 TR liquid scintillation analyzer.

The long-term viability of *C. heintzii* in the presence of neptunium was monitored by colony forming unit (cfu) plate counts. The 10-fold diluted subsamples described above were used to prepare serial dilutions up to 10^{-8}:1. Two 25-μL splits from each dilution were spread onto 1.8% agar–NTA growth media culture plates and observed for colony formation.

Extraction of particulate-associated neptunium was determined by two methods: via dilution by the addition of 0.1 mL of unfiltered sample to 0.9 mL of deionized water and via recomplexation by addition of 0.1 mL of unfiltered sample

TABLE 1. Equilibrium Formation Constants for Major Neptunium Aqueous Species in NTA Mineral Growth Medium

species	$\beta_{xyz}{}^a$	ref
NpO_2OH	$\beta_{1(-1)0} = 10^{-11.3}$	33, 34
$NpO_2(OH)_2{}^-$	$\beta_{1(-2)0} = 10^{-23.43}$	33, 34
$NpO_2CO_3{}^-$	$\beta_{101} = 10^{4.38}$	29, 30, 35
$NpO_2(CO_3)_2{}^{3-}$	$\beta_{102} = 10^{6.55}$	29, 30, 35
$NpO_2(CO_3)_3{}^{5-}$	$\beta_{103} = 10^{6.4}$	29, 30, 35
NpO_2NTA^{2-}	$\beta_{101} = 10^{6.80}$	36, 37
NpO_2HNTA^-	$\beta_{111} = 10^{1.77}$	36
$NpO_2(OH)NTA^{2-}$	$\beta_{1(-1)1} = 10^{-4.66}$	36
$NpO_2HPO_4{}^-$	$\beta_{111} = 10^{14.23}$	12
$NpO_2PO_4{}^{2-}$	$\beta_{101} = 10^{6.33}$	12

^{a} Where $\beta_{xyz} = [M_xH_yL_z]/[M]^x[H]^y[L]^z$ or $\beta_{x(-y)z} = [M_x(OH)_yL_z][H]^y/[M]^x[L]^z$.

to 0.9 mL of 0.001 M NTA solution. Colloidal/precipitate neptunium–phosphate characterization was performed by measuring the absorption spectra of 0.125 mM Np(V) in the mineral salts media without NTA during NaOH titration. A similar procedure was completed on a 0.125 mM Np(V)–20 mM H_3PO_4 solution for comparison. $NpO_2PO_4^{2-}$ and $NpO_2HPO_4^-$ species were characterized by comparison with their known absorption bands (12).

Samples for NTA concentration analysis were prepared by adding 0.2 mL of 0.2-μm filtered solution to 1 mL of 10^{-3} M HCl. NTA analyses were performed with a Dionex DX-500 ion chromatograph (IC). The IC was calibrated using freshly prepared NTA standards. NTA peak location was verified after sample analysis by spiking one sample with additional NTA and reanalyzing.

Chemical Speciation Calculations. All chemical equilibrium calculations were performed using CCBATCH, a computer code developed at Northwestern University to investigate the dynamics of coupled biological and chemical reactions in mixed waste subsurface environments. The exact modeling methodology is describe elsewhere (6). To summarize, the model is unique in that it explicitly couples biological electron donor and acceptor substrate consumption to competing chemical reactions in order to determine the effect of biological reactions on the fate of various components in the system. Currently, the model systematically considers the following competing subsurface reactions: acid/base, complexation, fixed-pH precipitation, biomass synthesis and decay, substrate utilization (contaminant degradation), and toxicity effects.

On the basis of user input information, the model calculates the equilibrium concentrations of all chemical species in the system, including the degradable form of the electron donor substrate at the initial pH and component concentrations. It uses a Newton–Raphson technique that combines the aqueous-phase mass balances with mass-action equilibrium expressions for all relevant acid/base and complexation reactions, and it can compute the equilibrium pH from the proton condition when the pH is not fixed.

To calculate the dominant neptunium speciation in the NTA growth medium, we considered the formation of 47 complexes from 16 components. The important neptunium aqueous species and their formation constants are shown in Table 1. Formation constants for nonactinide metal complexes and acid dissociation constants were taken from Morel and Hering (28) and corrected to 0.1 M ionic strength. Carbonate speciation was calculated by assuming Henry's law equilibrium between the aqueous and gas-phase CO_2 concentrations.

Results and Discussion

Neptunium Stability and Toxicity toward *Chelatobacter heintzii* in Glucose Growth Media. Neptunium–glucose
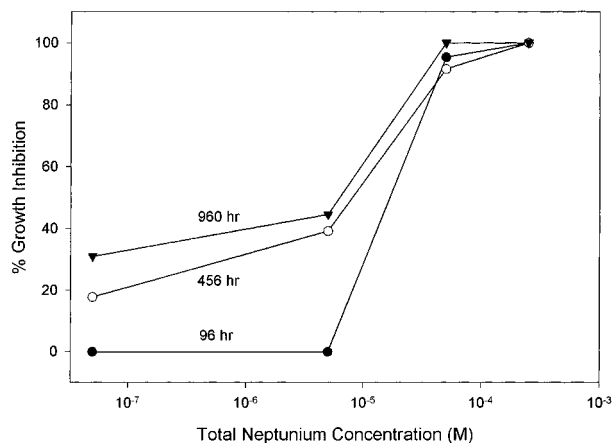
FIGURE 1. Effect of total neptunium concentration (M) on the relative growth of *Chelatobacter heintzii* in minimal glucose growth medium. The relative growth inhibition was calculated by normalizing the growth (OD_{600}) measurements of the neptunium containing samples to the growth observed in three control samples.

experiments were run at two different initial cell densities to determine if potential Np(V) toxicity was related to cell concentration. Microbial growth was tracked for all samples for 40 days. Within 24 h, cfu counts of the 2.5×10^{-4} M NpO_2^+ (the highest neptunium concentration investigated) samples showed a 51% loss in viability as compared to controls (data not shown). Figure 1 shows how the inhibition of *C. heintzii*, as determined by OD measurements over the course of the experiment, depended on the neptunium concentration. Within 96 h, samples exposed to the highest neptunium concentration (2.5×10^{-4} M) showed complete inhibition, while 5×10^{-5} M neptunium caused 95% inhibition after 96 h and complete inhibition after 960 h. A smaller inhibitory effect was observed after 480 h at the lowest neptunium concentration (5×10^{-8} M).

Chemical toxicity rather than radiolytic toxicity is the likely cause of the observed growth inhibition, since the damage caused by ionizing radiation dose-to-solution alone should be negligible at the Np concentrations used. While the lethal external radiation dose for *C. heintzii* is 330 Gy (33 KRad) (*24*), the actual dose at the highest concentration (2.5×10^{-4} M) was 0.1 Gy per day or only 4 Gy over the 40-day experiment. The relatively rapid onset of growth inhibition at NpO_2^+ concentrations $>5 \times 10^{-5}$ M further supports that neptunium inhibition was chemical, not radiolytic. Results for the Np–NTA system, reported below, also verify the conclusion of chemical toxicity.

Neptunium partitioning between aqueous and particulate phases was monitored in these experiments by absorption spectroscopy and α-scintillation counting of unfiltered vs 0.2-μm filtered samples. The NpO_2^+ concentrations determined from VIS–NIR spectroscopy indicated that the concentration of the Np(V) aquo species was stable over the course of the experiment. Scintillation counting showed that 0–20% of the ^{237}Np was associated with the particulate phase (data not shown). Since the most significant partitioning was measured in samples with high neptunium and biomass concentrations, we believe that the small amount of neptunium partitioning was an artifact of the filtration procedure rather than an indication of significant biosorption. We would not expect biosorption to be a significant mechanism in the Np(V) system since NpO_2^+ sorption on organic surfaces is much less significant than that of Pu(IV) due to the large difference in charge between the two ions (*10*).

Stability of the Np–NTA Complex during NTA Degradation. The growth rate of *C. heintzii* in NTA mineral media could be adversely affected by the presence of neptunium

in two ways. Because NTA is a strong chelator, most neptunium in solution will form a neptunium–NTA complex, effectively rendering a portion of the NTA unavailable for biological utilization. However, chemical equilibrium speciation calculations predict that even the highest concentration neptunium sample could only complex with ≈2% of the initial NTA in solution. Thus, the concentration-dependent growth rate of *C. heintzii* should remain unaffected by the amount of neptunium present in these experiments as long as sufficient excess NTA is present.

The second possible mechanism that could affect the biological growth rate is the potential toxicity of neptunium toward *C. heintzii*, either as a result of metal toxicity (free ion) or due to radiolytic (free or complexed neptunium) effects. Results from the neptunium–glucose experiments showed that significant metal toxicity would not be expected unless the concentration of the free Np(V) released from the NTA complex exceeded 5×10^{-5} M. To isolate potential radiotoxicity effects from neptunium chemical toxicity, the minimum starting NTA:neptunium ratio for these experiments was 50:1. Chemical speciation calculations indicated that the highest free NpO_2^+ concentration was 1.3×10^{-5} M under the initial conditions; therefore, the chemical toxicity effects from the free ion should have been small.

Figure 2 shows the growth of *C. heintzii* in NTA mineral media in the presence of increasing neptunium concentrations. Growth was unaffected by total neptunium concentrations up to 1.2×10^{-4} M, a result supported by cfu counts taken during the course of the experiments. Culture plates prepared from each sample at the end of the experiment showed that cells grown in the presence of all neptunium concentrations investigated had similar colony numbers to the control samples, verifying that radiotoxicity due to dose-to-solution was not important at these concentrations.

Previous work by Reed et al. (*24*) in the Pu(IV)–NTA system showed that radiolytic effects, due to preferential association of Pu(IV) with the biomass, were observed at radiation doses below the lethal dose. Figure 3 shows the amount of neptunium associated with *C. heintzii*. Partitioning to the solid phase was negligible for the first 250 h but then rapidly increased. At the end of the experiment, the amount of neptunium in the filtrate was roughly proportional to the total neptunium concentration in solution (data not shown).

Although the Pu(IV) associated with *C. heintzii* cells was not readily extractable with EDTA (*24*), 0.001 M NTA recovered 97% of the neptunium from the particulate fraction, verifying that the particulate neptunium was nearly completely recoverable. Approximately 41% of the particle-associated neptunium was extracted by 10-fold dilution with deionized water of one of the 10^{-4} M neptunium samples. The resulting particulate neptunium was 55%, which corresponds with the measured particulate neptunium in the 10^{-5} M neptunium sample. Therefore, the neptunium partitioning was reversible and concentration dependent within the short time frame of the extraction procedure, indicating that the free Np(V) ion concentration was reaching chemical equilibrium with the particulate fraction.

Neptunium Speciation during Glucose and NTA Biodegradation. Reversible, concentration-dependent partitioning and lack of microbial growth inhibition suggest that neptunium released from the NTA complex was being scavenged by other ligands in the system, making it unavailable to *C. heintzii*. Subsequent colloid formation or precipitation would explain neptunium association with the biomass. To determine the mechanism responsible for mitigating the potential toxicity of neptunium released from NTA complexation, chemical equilibrium modeling was combined with spectrophotometric investigations to establish the changing speciation of neptunium in the growth media during NTA degradation.
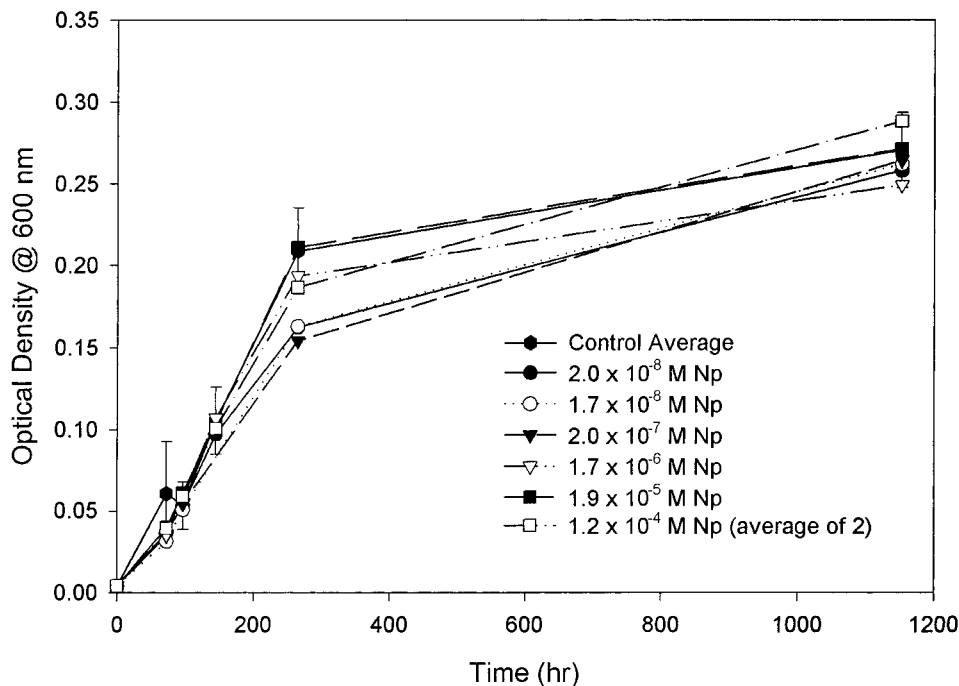
FIGURE 2. Growth of *C. heintzii* vs time in NTA mineral medium. Error bars are 99% confidence limits of the mean of three control samples. Total neptunium concentrations of up to 1.2×10^{-4} M had no significant effect on the growth of the organism when complexing ligands were present in solution.
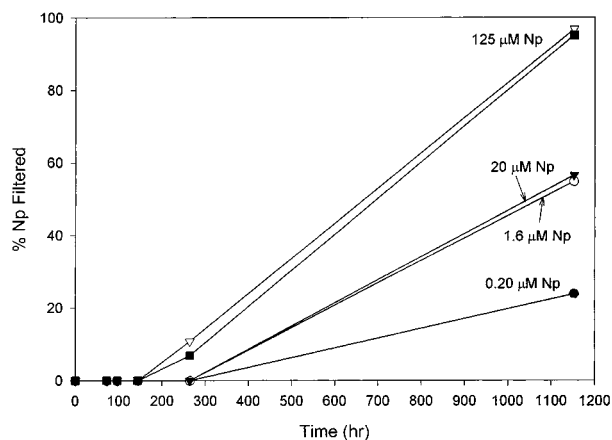

FIGURE 3. Neptunium partitioning during NTA degradation by *C. heintzii.* Partitioning was determined by α-particle scintillation count comparison of filtered to unfiltered samples.

VIS−NIR spectroscopy during the glucose media experiments verified that the Np(V) oxidation state is stable at neutral pH in the presence of *C. heintzii.* The stability of the Np(V)−NTA complex was monitored by periodically measuring the absorption spectrum during NTA degradation by *C. heintzii.* Figure 4a compares spectra from a 1.25×10^{-4} M neptunium−NTA sample after 2 h and 3, 4, 6, and 48 days of growth. The complex was initially stable in the presence of biological activity for up to 6 days. Loss of the neptunium−NTA complex from solution at 48 days is reflected by the disappearance of the absorption band at 990.2 nm.

Two possible explanations can account for the association of neptunium with the biomass following NTA degradation by *C. heintzii.* First, free NpO_2^+ may have been adsorbed onto the cell membrane, as is seen in the Pu system. However, results from glucose−media experiments suggested that biosorption of neptunium is not a significant process. An alternative explanation is that neptunium released from the NTA complex could have formed a solid phase if NTA degradation by *C. heintzii* changed the solution character-

istics such that neptunium precipitation became favorable. Figure 4b shows an enlargement of the 48-day spectrum of the unfiltered 10^{-4} M neptunium sample shown in Figure 4a. The unfiltered spectrum shows new band formation at ≈ 1015 nm, which is indicative of the formation of a new neptunium species.

Precipitate formation should be correlated with the loss of NTA from solution, since excess NTA would lead to a stable NTA complex. The small 990-nm peak for a filtered sample, shown in the inset of Figure 4b, corresponded to the final concentration of NTA at the end of the experiment, shown in Table 2, and the maximum amount of neptunium that could be complexed by NTA. All samples showed nearly complete NTA degradation, verifying that neptunium speciation was no longer being dominated by NTA complexation.

The 1015-nm peak observed in Figure 4, panels a and b, has not been previously reported for Np(V) VIS−NIR absorption spectra. However, carbonate and phosphate complexation with Np(V) are known to cause red-shifted new band formation in the VIS−NIR. Carbonate is present in groundwater as a byproduct of organic degradation and as a result of mineral dissolution, and it is a strong actinide complexant that can affect actinide mobility in subsurface aquifers (*29*). Neptunium solubility in many carbonate systems is controlled by a $Me(I)NpO_2CO_3$ precipitate, where Me(I) represents any monovalent cation. Using a representative solubility product of $10^{-10.28}$ (*30*), the expected NpO_2^+ concentration in equilibrium with a $Me(I)NpO_2CO_3$ solid, 0.1 M Me(I), and atmospheric $CO_2(g)$ at pH 8, the highest final pH of the growth media after NTA degradation, would be $\approx 2.6 \times 10^{-4}$ M. All the final measured NpO_2^+ concentrations shown in Table 2 were below this level, suggesting that neptunium solubility was being controlled by another solid phase.

Chemical equilibrium calculations by Morgenstern and Kim (*12*) have shown that phosphate complexation with neptunium can out-compete carbonate complexation in natural waters when phosphate concentrations exceed 10^{-4} M. Although phosphate solid phases have been characterized for some actinide systems, no quantitative solubility data are available for the Np(V)−phosphate system.
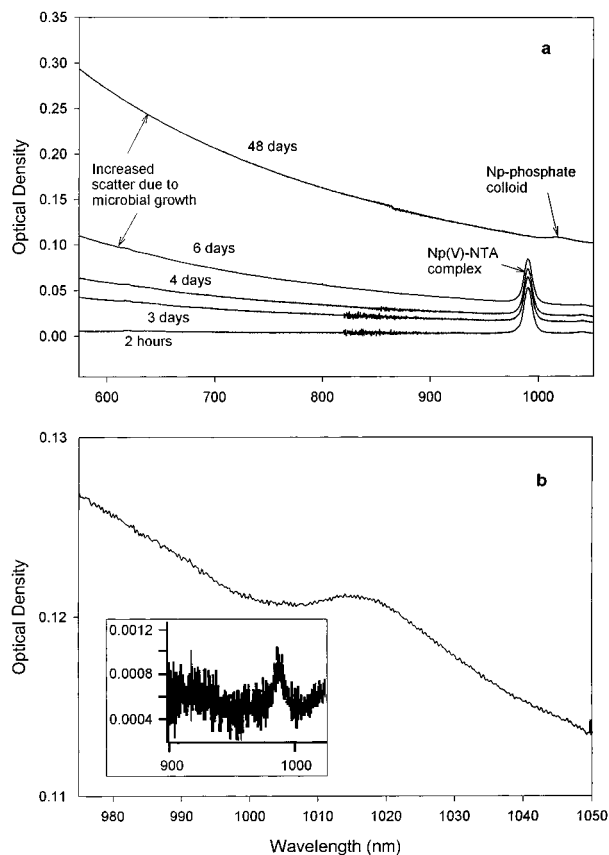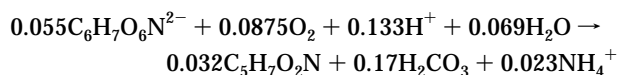
FIGURE 4. VIS—NIR spectra of 1.25×10^{-4} M neptunium in NTA mineral media during NTA degradation by *C. heintzii*, showing the stability of the neptunium—NTA complex (990.2 nm peak) and microbial growth (OD_{600}). (a) After NTA degradation, neptunium speciation shifted to the phosphate system, indicated by the 1015-nm absorption band. (b) Enlargement of the 970—1050-nm region of the unfiltered 48-day spectrum shown in panel a. The 1015-nm peak is clearly visible. A small amount of neptunium—NTA complex was seen after filtration (990-nm peak, inset).
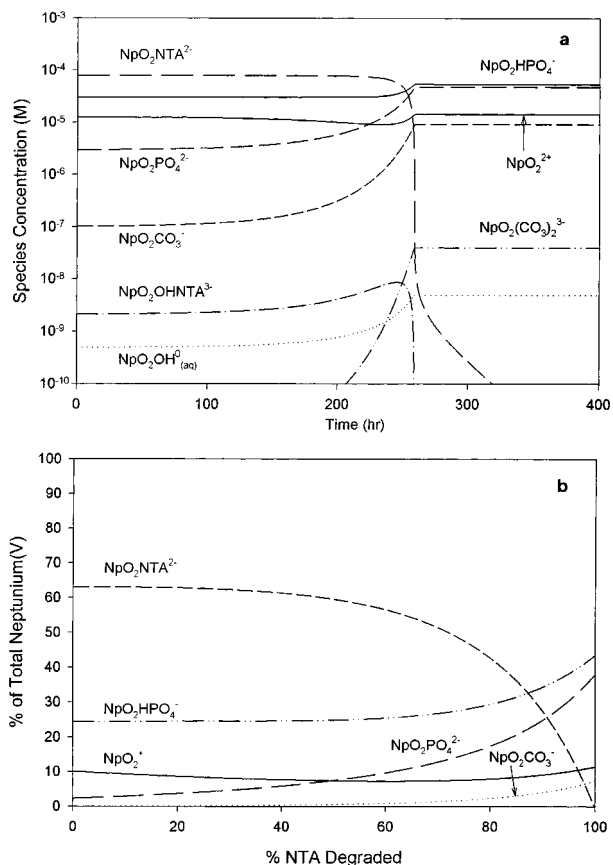
FIGURE 5. (a) Neptunium speciation during NTA degradation for 0.125 mM Np(V) in NTA mineral growth media, calculated by the dynamic chemical equilibrium computer code, CCBATCH. Calculations are based on equilibrium with $10^{-2.7}$ atm $CO_2(g)$ partial pressure and the assumption that no solid phases are present. (b) Calculated dominant neptunium complexes in the mineral growth medium as a function of amount of NTA degraded. $NpO_2HPO_4^-$ and $NpO_2PO_4^{2-}$ are the dominant neptunium species following NTA degradation, accounting for 80% of the total neptunium. The $NpO_2CO_3^-$ species accounted for less than 10% of the total neptunium in solution after NTA degradation.

TABLE 2. Final NTA and Neptunium Concentrations of Filtered NTA Growth Medium Samples after 48 Days[a]

initial Np(V) concn (M)	final Np(V) concn (M)	final NTA concn (M)	final pH
1.2×10^{-4}	3.8×10^{-6}	1.04×10^{-6}	7.90×0.03
1.2×10^{-4}	6.4×10^{-6}	2.91×10^{-6}	7.98×0.04
1.9×10^{-5}	8.3×10^{-6}	ND^b	7.83×0.03
1.7×10^{-6}	7.7×10^{-7}	ND	7.87×0.04
2.0×10^{-7}	1.5×10^{-7}	ND	7.73×0.03
1.7×10^{-8}	1.7×10^{-8}	7.97×10^{-7}	7.63×0.03
2.0×10^{-8}	2.0×10^{-8}	ND	7.84×0.02

[a] NTA concentrations determined by IC analysis. Neptunium determined by α-particle scintillation counting. [b] ND, not detected ($<1 \times 10^{-7}$ M).

To predict the dominant neptunium complexes in the system, we used the computer program CCBATCH to simulate the equilibrium chemical speciation of the mineral growth media during NTA degradation by *C. heintzii*. The aerobic biodegradation of NTA can be described by the following stoichiometry when $HNTA^{2-}$ is selected as the degradable form of NTA (*6, 8*):

$$0.055C_6H_7O_6N^{2-} + 0.0875O_2 + 0.133H^+ + 0.069H_2O \rightarrow$$
$$0.032C_5H_7O_2N + 0.17H_2CO_3 + 0.023NH_4^+$$

where $C_5H_7O_2N$ represents biomass.

Inspection of the reaction stoichiometry explains the pH rise observed in weakly buffered systems undergoing NTA degradation. Each mole of $HNTA^{2-}$ degraded consumes 2.4 acid equivalents, causing the rise in pH. The magnitude of this effect depends on the concentration of other buffers in the system and may also be mitigated by retention in solution of a portion of the 3.4 mol of carbonic acid produced per mole of NTA degraded. For example, in a closed system, carbonic acid retention causes a less dramatic pH increase as compared to a solution in equilibrium with atmospheric $CO_2(g)$. Additionally, precipitation of $Np-CO_3^{2-}$ or $-PO_4^{2-}$ solids would remove base equivalents from the system at near-neutral pH, which could also counter increasing pH.

The final pH measurements for all the neptunium—NTA samples are shown in Table 2. As predicted by the degradation stoichiometry, consumption of NTA caused a 0.6—1 pH unit increase. Modeling studies of the growth medium speciation in equilibrium with atmospheric $CO_2(g)$ partial pressures ($10^{-3.5}$ atm) yielded a final pH prediction of 8.5, indicating that pH was being affected by carbonic acid retention and/or precipitation of base equivalents. Figure 5a shows the predicted dominant speciation of the 0.125 mM Np(V)—NTA mineral media solution in equilibrium with a slightly elevated $CO_2(g)$ partial pressure of $10^{-2.7}$ atm, which yielded a final predicted pH of 7.9. The modeling results show that $NpO_2HPO_4^-$ and $NpO_2PO_4^{2-}$ are the dominant
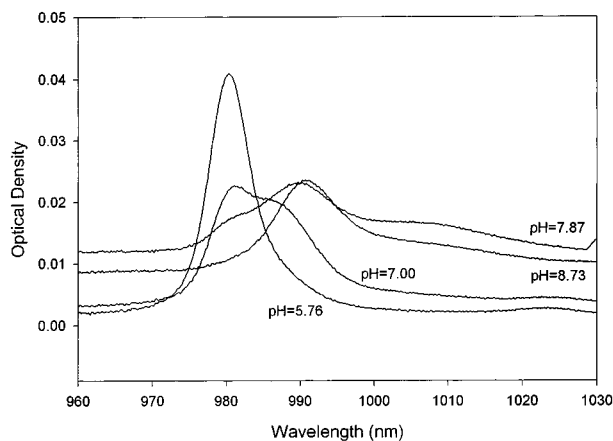
FIGURE 6. VIS−NIR absorption spectra of 0.125 mM Np(V) in NTA-free mineral salts growth media at various pH. The dominant neptunium species in solution are NpO_2^+ [980.2 nm (*25*)], $NpO_2HPO_4^-$ [988.8 nm (*12*)], and $NpO_2PO_4^{2-}$ [993.6 nm (*12*)]. Spectra matched those obtained for a 20 mM H_3PO_4 solution (not shown).

neptunium species after significant NTA degradation has taken place. This prediction is consistent with our absorption spectra, which did not show evidence of significant Np−carbonate complexation. Additionally, the final NpO_2^+ ion concentration calculated by the model, 1.4×10^{-5} M, exceeds the final measured concentrations in Table 2, indicating that solubility of a neptunium solid phase is limiting the amount of neptunium in solution.

Figure 5b shows the model-predicted distribution of neptunium among the major complexing ligands during NTA degradation at $10^{-2.7}$ atm $CO_2(g)$ partial pressure. It illustrates that phosphate complexation accounts for 80% of the neptunium speciation in solution after complete NTA degradation. Consequently, we attempted to experimentally correlate the 1015-nm peak formation with the phosphate system. To identify the 1015-nm peak, the variable-pH VIS−NIR spectra of Np(V) in the defined mineral salts media (without any NTA) were compared to the Np(V) spectra obtained in a 20 mM H_3PO_4 solution. The behavior of both systems followed the results seen by Morgenstern and Kim (*12*) in lower concentration phosphate solutions: Figure 6 shows that as pH was increased, neptunium speciation shifted from the free aquo species to successive complexation as $NpHPO_4^-$ ($\approx$988 nm) and $NpPO_4^{2-}$ ($\approx$993 nm). Figure 7 shows that, after $\approx$20 min, new band formation at 1015 nm was observed at the expense of the $NpPO_4^{2-}$ complex, and the overall turbidity of both solutions increased, suggesting colloid formation/precipitation. The final spectrum remained stable for 3 days (Figure 7), but the colloidal species had to be resuspended in solution prior to each spectroscopic analysis. These results indicate that neptunium speciation after NTA degradation was controlled by the phosphate system and that neptunium−phosphate colloid formation/precipitation can be identified by VIS−NIR peak formation at 1015 nm.

Our results correlate with work by Francis et al. (*19*), who showed that nickel toxicity was modulated by coprecipitation of Ni with iron hydroxides after citrate degradation. Also, formation of a neptunium−phosphate colloidal/precipitate phase agrees with results reported for the Np(V) and Pu(VI) systems (*13, 31, 32*), suggesting that phosphate colloid formation/precipitation may be an important mechanism affecting actinide solubility and speciation in natural systems. This latter finding will be investigated further since phosphorus is a required biological nutrient and many in-situ bioremediation efforts require supplemental phosphorus additions.
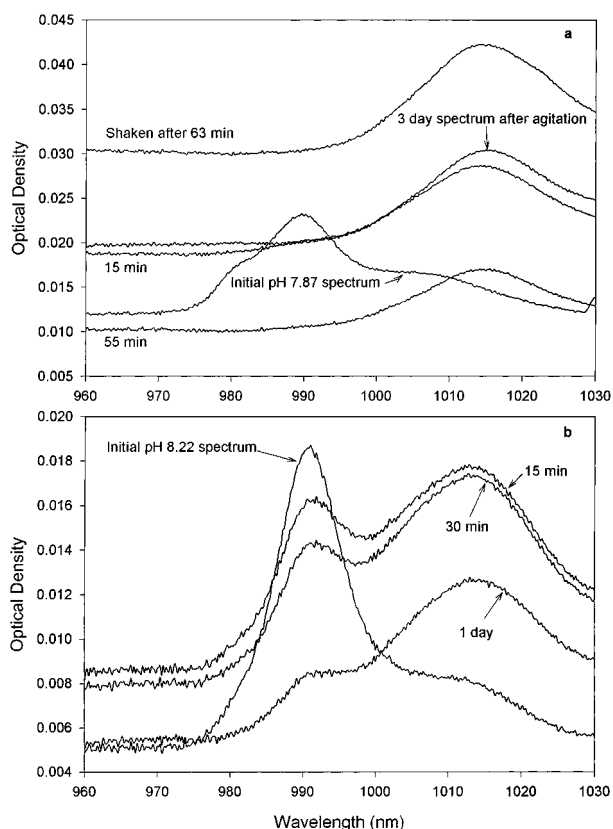

FIGURE 7. VIS−NIR absorption spectra of 0.125 mM Np(V) in NTA-free mineral salts growth media at pH 7.87 (a) and in a 20 mM H_3PO_4 solution at pH 8.22 (b), both as a function of time. Predominant neptunium speciation shifts from phosphate complexation to an unidentified colloidal/precipitate phase (1015 nm) that remained stable for several days. Note the increase in solution turbidity (baseline OD_{960} shift from 0.011 to 0.031) caused by agitation.

Our results in this study are in contrast to previous findings in the plutonium−NTA system (*24*), where *C. heintzii* was sensitive to radiolytic effects at similar actinide concentrations due to selective association of plutonium with the biomass and the higher specific activity of ^{239}Pu. This work suggests that future bioremediation efforts involving actinide elements will require careful evaluation of coupled chemical, radiolytic, and biological processes.

Acknowledgments

Literature Cited

(1) Riley, R. G.; Zachara, J. M.; Wobber, F. J. *Chemical Contaminants on DOE lands and Selection of Contaminant Mixtures for Subsurface Science Research*; U.S. Department of Energy Report DOE/ER-0547T; Office of Energy Research: 1992.

(2) Baik, M. H.; Lee, K. J. *Ann. Nucl. Energy* **1994**, *21*, 81−96.

(3) Jardine, P. M.; Jacobs, G. K.; O'Dell, J. D. *Soil Sci. Soc. Am. J.* **1993**, *57*, 954−962.

(4) Means, J. L.; Crerar, D. A.; Duguid, J. O. *Science* **1978**, *200*, 1477−1481.

(5) Broido, M. S. *Natural and Accelerated Bioremediation Research (NABIR)*; U. S. Department of Energy Report DOE/ER-0659T; 1995.

(6) Rittmann, B. E.; VanBriesen, J. M. In *Reviews in Mineralogy*; Lichtner, P. C., Steefel, C. I., Oelkers, E. H., Eds.; Mineralogical Society of America:, 1996; Vol. 34: Reactive Transport in Porous Media.

(7) Egli, T. In *Biochemistry of Microbial Degradation*; Ratledge, C., Ed.; Kluwer: Dordrecht, 1994.

(8) Bolton, H. J.; Girvin, D.; Plymale, A.; Harvey, S.; Workman, D. *Environ. Sci. Technol.* **1996**, *30*, 931−938.

(9) Lieser, K. H. *Radiochim. Acta* **1995**, *70/71*, 355−375.

(10) Silva, R. J.; Nitsche, H. *Radiochim. Acta* **1995**, *70/71*, 377−396.

(11) Stumm, W.; Morgan, J. J. *Aquatic Chemistry*, 3rd ed.; John Wiley & Sons, Inc.: New York, 1996.

(12) Morgenstern, A.; Kim, J. I. *Radiochim. Acta* **1996**, *72*, 73−77.

(13) Nash, K. L.; Morss, L. R.; Jensen, M. P.; Schmidt, M. *Phosphate Mineralization of Actinides by Measured Addition of Precipitating Anions*; Chemistry Division, Argonne National Laboratory Report CH2-6-C3-22; 1996.

(14) Macaskie, L. E.; Jeong, B. C.; Tolley, M. R. *FEMS Microbiol. Rev.* **1994**, *14*, 351−368.

(15) Macaskie, L. E.; Empson, R. M.; Lin, F.; Tolleys, M. R. *J. Chem. Technol. Biotechnol.* **1995**, *63*, 1−16.

(16) Macaskie, L. E.; Lloyd, J. R.; Thomas, R. A. P.; Tolley, M. R. *Nucl. Energy* (*Br. Nucl. Energy Soc.*) **1996**, *35*, 257−271.

(17) Babich, H.; Stotzky, G. In *Advances in Applied Microbiology*; Laskin, A. I., Ed.; Academic Press: New York, 1983; Vol. 29.

(18) Collins, Y.; Stotzky, G. In *Metal Ions and Bacteria*; Beveridge, T. J., Doyle, R. J., Eds.; John Wiley and Sons, Inc: New York, 1989.

(19) Francis, A. J.; Joshi-Topé, G. A.; Dodge, C. *Environ. Sci. Technol.* **1996**, *30*, 562−568.

(20) Markich, S. J.; Brown, P. L.; Jeffree, R. A. *Radiochim. Acta* **1996**, *74*, 321−326.

(21) Mattimore, V.; Udupa, K. S.; Berne, G. A.; Battista, J. R. *J. Bacteriol.* **1995**, *177*, 5232−5237.

(22) Ewing, D. In *Radiation Chemistry: Principles and Applications*; Farhataziz, Rodgers, M. A. J., Eds.; VCH Publishers: New York, 1987.

(23) Wildung, R. E.; Garland, T. R. *Appl. Environ. Microbiol.* **1982**, *43*, 418−423.

(24) Reed, D. T.; Vojta, Y.; Quinn, J. W.; Richmann, M. K. *Radiochim. Acta* Submitted for publication.

(25) Fahey, J. A. In *The Chemistry of the Actinide Elements*, 2nd ed.; Katz, J. J., Seaborg, G. T., Morss, L. R., Eds.; Chapman and Hall: New York, 1986; Vol. 1.

(26) Tiedje, J. M.; Mason, B. B.; Warren, C. B.; Malec, E. J. *Appl. Microbiol.* **1973**, *25*, 811−818.

(27) Bally, M.; Wilberg, E.; Kuhni, M.; Egli, T. *Microbiology* (*Reading, U.K.*) **1994**, *140*, 1927−1936.

(28) Morel, F. M. M.; Hering, J. G. *Principles and Applications of Aquatic Chemistry*; John Wiley & Sons: New York, 1993.

(29) Clark, D. L.; Hobart, D. E.; Neu, M. P. *Chem. Rev.* **1995**, *95*, 25−48.

(30) Neck, V.; Runde, W.; Kim, J. I.; Kanellakopulos, B. *Radiochim. Acta* **1994**, *65*, 29−37.

(31) Weger, H. T.; Okajima, S.; Cunnane, J. C.; Reed, D. T. *Bulk Solubility and Speciation of Plutonium*(*VI*) *in Phosphate-Containing Solutions*; Argonne National Laboratory Report ANL-CMT-CP-78233; 1993.

(32) Weger, H. T. Ph.D. Thesis, University of Illinois, Champaign−Urbana, IL, 1994.

(33) Neck, V.; Kim, J. I.; Kanellakopulos, B. *Radiochim. Acta* **1992**, *56*, 25−30.

(34) Lierse, C.; Treiber, W.; Kim, J. I. *Radiochim. Acta* **1985**, *38*, 27−28.

(35) Bidoglio, G.; Tanet, G.; Chatt, A. *Radiochim. Acta* **1985**, *38*, 21−26.

(36) Eberle, S. H.; Wede, U. *J. Inorg. Nucl. Chem.* **1970**, *32*, 109−117.

(37) Nitsche, H.; Becraft, K. In *Transuranium Elements−A Half Century*; L. R. Morss, Fuger, J., Eds.; American Chemical Society: Washington, DC, 1992.